Thermochimica Acta 503–504 (2010) 16–20

Contents lists available at ScienceDirect

Thermochimica Acta

journal homepage: www.elsevier.com/locate/tca

# Thermal behavior and decomposition of kaolinite–potassium acetate intercalation composite

Hongfei Cheng[a,b,c], Qinfu Liu[a], Jing Yang[c], Qian Zhang[d], Ray L. Frost[c,*]

[a] School of Geoscience and Surveying Engineering, China University of Mining & Technology, Beijing 100083, China
[b] School of Mining Engineering, Inner Mongolia University Of Science & Technology, Baotou 014010, China
[c] Inorganic Materials Research Program, School of Physical and Chemical Sciences, Queensland University of Technology, 2 George Street, GPO Box 2434, Brisbane, Queensland 4001, Australia
[d] School of Materials Science and Engineering, Henan Polytechnic University, Jiaozuo 454000, China

ARTICLE INFO

*Article history:*
Received 8 December 2009
Received in revised form 11 February 2010
Accepted 14 February 2010
Available online 3 March 2010

*Keywords:*
Kaolinite
Potassium acetate
Intercalation
Thermal behavior
Decomposition

ABSTRACT

A series of kaolinite–potassium acetate intercalation composite was prepared. The thermal behavior and decomposition of these composites were investigated by simultaneous differential scanning calorimetry–thermogravimetric analysis (DSC–TGA), X-ray diffraction (XRD) and Fourier transformation infrared (FT-IR). The XRD pattern at room temperature indicated that intercalation of potassium acetate into kaolinite causes an increase of the basal spacing from 0.718 to 1.428 nm. The peak intensity of the expanded phase of the composite decreased with heating above 300 °C, and the basal spacing reduced to 1.19 nm at 350 °C and 0.718 nm at 400 °C. These were supported by DSC–TGA and FT-IR results, where the endothermic reactions are observed between 300 and 600 °C. These reactions can be divided into two stages: (1) removal of the intercalated molecules between 300 and 400 °C. (2) dehydroxylation of kaolinite between 400 and 600 °C. Significant changes were observed in the infrared bands assigned to outer surface hydroxyl, inner surface hydroxyl, inner hydroxyl and hydrogen bands.



## 1. Introduction

Kaolinite, with the chemical composition $Al_2Si_2O_5(OH)_4$, is the most abundant mineral of the kaolin group including dickite, nacrite and halloysite, and is a dioctahedral 1:1 phyllosilicate formed by superposition of silicon tetrahedral sheets and aluminum octahedral sheets. Adjacent layers are linked by van der Waals forces and hydrogen bonds. This interlayer induces restricted access to the interlamellar aluminol groups (Al–OH) that may be used for grafting reactions. The most reactive functional groups in kaolinite are hydroxyl groups, which are capable of taking part in many chemical reactions as well as ion exchange processes [1].

Kaolinite is a frequently studied clay mineral noted for its unique physiochemical characteristics and versatile industrial applications [1]. Therefore, the variety of industrial applications has motivated a vigorous research effort which has revealed concurrent dramatic enhancements for many materials. Kaolinite is commonly used for the production of composites which exhibit unexpected hybrid properties, e.g. enhanced mechanical, thermal, dimensional and barrier performance properties as well as flame retardant characteristics etc [2–4]. In particular, one of the most studied systems to date is the intercalation of synthetic polymers within layered aluminosilicates [5–7]. While being intercalated within the inorganic structure, organic polymers naturally reduce their structural mobility and some of them assume a highly organized conformation within the layered structure. In this way, it is possible to produce nanocomposites that usually present unique properties compared to the corresponding properties of the isolated starting materials and/or their mechanical blends [8]. The composite of kaolinite intercalated by organic molecules have gained much attention over the last decades, essentially making the clay into a single layered mineral [9–13]. The layered kaolinite particles were intercalated with small molecules, such as urea, potassium acetate, dimethylsulphoxide, and so on, to expand the interlayer space, thereby allowing the interlayer hydroxyl group to be accessed by organic molecules [14–17]. The inserting molecule breaks the hydrogen bonds formed between the kaolinite hydroxyl groups and the oxygens of the next adjacent siloxane layer, then forms hydrogen bonds with either the hydrophobic surface of the kaolinite (the siloxane layer) or the hydrophilic part of the kaolinite surface (the hydroxyl surfaces of the gibbsite-like layer). A further possibility exists in that the inserting or adsorbing molecule may interact with the end surfaces of the kaolinite [18].

In the case of application of intercalated kaolinite, heating treatment is somewhat necessary especially as filler in plastic and rubber. Regarding of this, the study of thermal stability of potas-

* Corresponding author. Tel.: +61 7 3138 2407; fax: +61 7 3138 1804.
*E-mail address:* r.frost@qut.edu.au (R.L. Frost).

0040-6031/$ – see front matter © 2010 Elsevier B.V. All rights reserved.
doi:10.1016/j.tca.2010.02.014

sium acetate intercalation kaolinite is interesting. In current study, the combination of thermal analysis, X-ray diffraction and infrared spectroscopy is used to investigate the changes in the composite of kaolinite intercalated by potassium acetate.

## 2. Experimental methods

### 2.1. Materials

The sample used in this study was the natural pure kaolin from Zhangjiakou Hebei province of China, with size of 45 μm. Its chemical composition in wt% is $SiO_2$ 44.64, $Al_2O_3$ 38.05, $Fe_2O_3$ 0.22, MgO 0.06, CaO 0.11, $Na_2O$ 0.27, $K_2O$ 0.08, $TiO_2$ 1.13, $P_2O_5$ 0.13, MnO 0.002, loss on ignition 15.06. The major mineral constituent is well ordered kaolinite (95 wt%) with a Hinckley index of 1.31. The potassium acetate (A. R) was purchased from Beijing Chemical Reagents Company, China.

### 2.2. The intercalation composite preparation

The potassium acetate (KAc) intercalates was prepared by immersing 10 g of kaolinite in 20 ml of KAc solution at a mass percentage concentration of 30%, stirring for 10 min. The composite was allowed to dry at room temperature before the DSC–TGA, XRD and FT-IR analysis.

### 2.3. Characterization

The simultaneous DSC–TGA measurements were performed by using American TA Instruments SDT Q600 under $N_2$ (100 ml $min^{-1}$) at a heating rate of 10 °C $min^{-1}$. About 15 mg sample was placed in alumina crucibles and heated from room temperature to 1080 °C.

The powder X-ray diffraction (XRD) analysis was performed using a Japan Rigaku D/max-rA X-ray diffractometer (40 kV, 100 mA) with Cu (λ = 1.54178 Å) irradiation at the scanning range of 2.6–50°.

Fourier transform infrared (FT-IR) spectroscopic analysis was undertaken using a NICOLET 750 SX spectrometer. FT-IR spectra between 600 and 4000 $cm^{-1}$ were obtained. The samples were prepared at KBr pellets (ca. 2% by mass in KBr).

## 3. Results and discussion

### 3.1. Thermal analysis

Thermal analysis can reveal information about the thermal behavior of intercalated kaolinite [18,19]. Fig. 1a displays the results of the DSC–TGA curves of kaolinite and clearly shows a peak at 527 °C corresponding to its dehydroxylation in addition to an exothermic peak at 998 °C associated with the formation of a spinel phase that was transformed into mullite [20–23]. However, there are two endothermic peaks at 76, 373 °C for the intercalation composite in Fig. 1b. It is therefore concluded that the endothermic peak at 76 °C results from removing of the adsorbed water on the composite, and the endothermic peak at 373 °C results from the decomposition of the potassium acetate in the layer of expanded kaolinite.

The strong decrease between 300 and 400 °C is related to the intercalated molecules (Fig. 1b). The intercalation composite was formed from the expansion of kaolinite with both potassium acetate and water [12,24], so this strong decrease is the decomposition of the potassium acetate and water in the layer of kaolinite. The water associated with KAc and $Al^{3+}$–OH was removed before 350 °C and the KAc between the layers of kaolinite was decomposed. The jump close to 400 °C was interpreted as decarboxylation of acetate [23]. Both the derivative thermogravimetric (DTG) and TGA curves

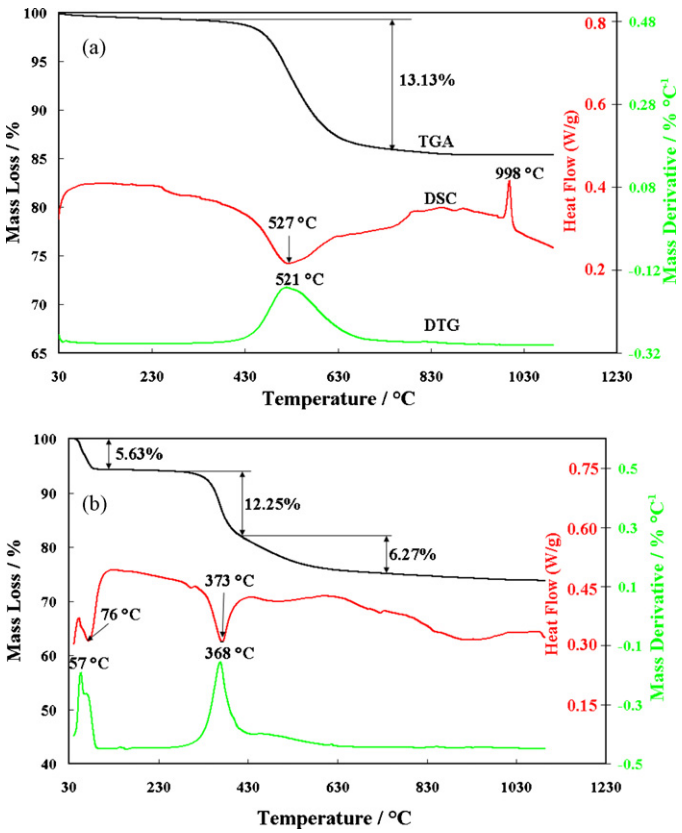


**Fig. 1.** DSC–TGA curves of (a) kaolinite and (b) the kaolinite–potassium acetate intercalation composite.

show weight losses at 76, 373 °C for the composite, and only one weight loss at 527 °C for untreated kaolinite.

The thermoanalytical investigations revealed that the kaolinite–KAc composite is stable at least up to 300 °C. Decomposition of the intercalated composite begins after the melting of the KAc intercalated in the interlayer spaces, indicating that the reactions occur in the presence of a molten salt [22,25]. The maximum rate of mass loss of the intercalation composite is observed at 373 °C, instead of 527 °C, for the pure kaolinite sample. Thus this is benefit to the calcinations. Reactions in the presence of a molten phase are rather composite processes (e.g. the formation and reduction by elemental carbon of $K_2CO_3$ and the formation of $KAlSiO_4$) [22]. The DSC curve at 998 °C indicates no spinel phase that was transformed into mullite of the intercalated sample. Probably the obtained solid potassium compound prohibits the formation of a crystalline spinel phase [22,26].

### 3.2. X-ray diffraction

When the kaolinite was intercalated with KAc, expansion occurred along the *C*-axis only [27]. Fig. 2 shows the XRD patterns of kaolinite and its intercalated composite with KAc. The XRD pattern shows that the basal $d_{(0\,0\,1)}$ of kaolinite expands from 0.718 to 1.428 nm; The increment of 0.71 nm in *d*-value of kaolinite indicates the intercalation of KAc in the interlamellar space, which is consistent with the results published before [9,28,29]. The loss of intensity of composite in the $d(0\,2\,2)$, $d(1\,\bar{3}\,0)$, $d(\bar{1}\,3\,1)$, $d(0\,0\,3)$, $d(1\,\bar{3}\,1)$ and $d(\bar{1}\,1\,3)$ peaks suggest that the well crystallized kaolinite suffers structural degradation after intercalation.

In order to analyze the thermal stability of KAc intercalated kaolinite composite, the samples were heated under specific temperatures at 150, 200, 250, 300, 350 and 400 °C for 2 h. Their

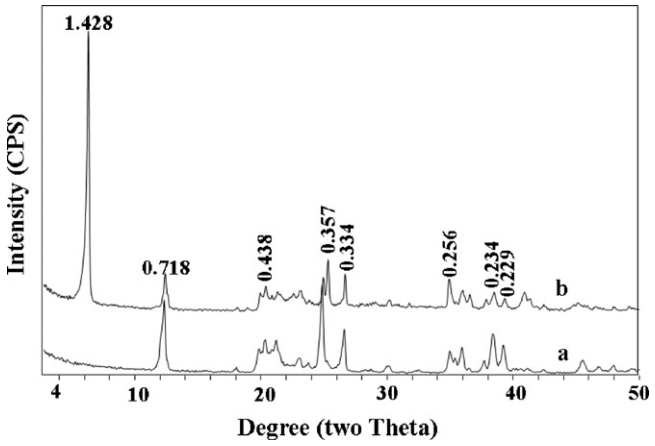


**Fig. 2.** X-ray diffraction (XRD) patterns of (a) kaolinite and (b) kaolinite/potassium acetate composite.

XRD patterns are shown in Fig. 3. Although the peak for 1.428 nm was attributed to the intercalated phase, the area of the 0.718 nm peak cannot be fully attributed to the non-intercalated kaolinite because the weak 0 0 2 peak of the intercalated kaolinite was located at 0.714 nm nearby the 0.718 nm peak in Fig. 3a–c [28]. The XRD patterns obtained between 150 and 250 °C (Fig. 3b–d) reveal that the modifications are scarce at this temperature range, where the composite reflections remain unchanged. This phase with the largest $d_{(0\,0\,1)}$ spacing is the fully expanded by water and potassium acetate before 250 °C. Upon heating to 300 °C, the composite starts to deintercalate and the water coordinated to KAc was also lost. The dehydration of the intercalation composite through heating results the 1.190 nm phase. The difference between the 1.19 nm and 0.718 nm phases is attributed to the loss of the KAc in the layer of the composite. Partial removal of the intercalated molecules begins between 300 and 350 °C, as indicated by reduction of the basal spacing of the composite from 1.428 to 1.190 nm. Both the 1.428 and the 1.190 nm reflections are visible in the pattern obtained at 300 °C. The difference between the two phases of 0.23 nm is attributed to the loss of water and this value is approximately the size of molecular water. After heating above 400 °C, no intensity of the 1.428 nm *d*-spacing remained and the intensity of the 0.718 nm peak start to increase.

Heating between 300 and 400 °C (Fig. 3e–h) causes the shift of the basal reflections of the composite from 1.428 to 1.190 nm (Fig. 3h). This reduction is, on the basis of the DSC–TGA data, caused by loss of some of the intercalated species. This probably due to the structural rearrangement caused by the loss of water coordinated to KAc molecule. In their structural model, KAc coordinated to water molecules serve as molecular props between the kaolinite layers, resulting in the observed 1.428 nm spacing. Partial loss of water drives the remaining KAc molecules into the ditrigonal holes of the oxygen-atom surface of the 1:1 layer, resulting in the 1.190 nm and 1.428 nm spacing that coexist at 350 °C.

After heating between room temperature and 400 °C, two main changes were observed. Two phases at 1.428 and 1.190 nm are observed within the KAc intercalated kaolinite. It can be concluded that the 1.428 nm peak in the KAc intercalated kaolinite results from the acetate coordinated to water. The 1.190 nm peak results from only KAc in the layer of kaolinite. This is the major phase at the elevated temperatures for the KAc intercalated kaolinite.

### 3.3. Infrared spectroscopy

The hydroxyl deformation modes of kaolinite are important in the spectroscopic analysis for the deintercalation of KAc intercalated kaolinite [30]. There are four kinds of hydroxyl groups in kaolinite, i.e. outer surface hydroxyl, inner surface hydroxyl, inner hydroxyl and absorbed water hydroxyl [11,19,27,31]. The inner hydroxyls are below the aluminium atoms and extend towards the intralayer cavity (vacant octahedral site) of the kaolinite [31–33].

Fig. 4 shows the FT-IR spectroscopy of high frequency region of the kaolinite–KAc intercalation composite, which were preheated at 150 and 200 °C, as well as at 250, 300, 350 and 400 °C. These temperature values were based on the DSC–TGA curves (Fig. 1). In the case of kaolinite (Fig. 6a), the four OH bands represent stretching vibration frequencies at 3692, 3668, 3651, and 3620 $cm^{-1}$, which are attributed to inner surface hydroxyl, outer surface hydroxyl, absorbed water hydroxyl and inner hydroxyl, respectively. The region of 3000–4000 $cm^{-1}$ presents a band at 3620 $cm^{-1}$, which is typical of the stretching of the internal OH groups in the kaolinite structure, and a band at 3692 $cm^{-1}$, which is characteristic of the vibration surface of OH groups [11,19,28,34]. In addition to the four OH bands, a new (hydrogen-bonded) band appeared at 3604 $cm^{-1}$, which are assigned to the formation of the hydrogen bonding of the inner surface hydroxyls and the acetate ion [35]. The acetate ion may interact with the kaolinite surfaces through

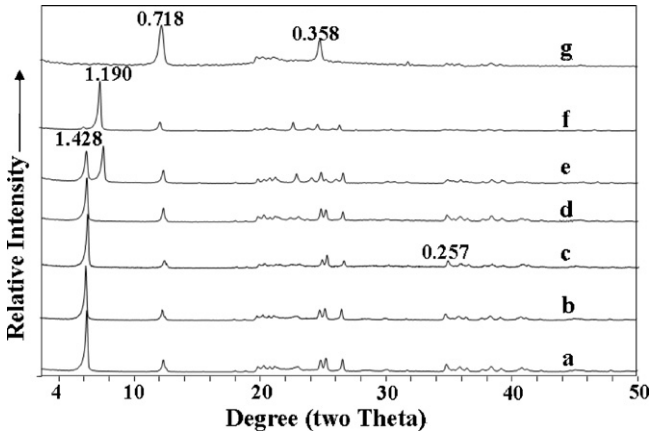


**Fig. 3.** XRD patterns of heating the kaolinite/potassium acetate composite at (a) room temperature, (b) 150 °C, (c) 200 °C, (d) 250 °C, (e) 300 °C, (f) 350 °C and (g) 400 °C.

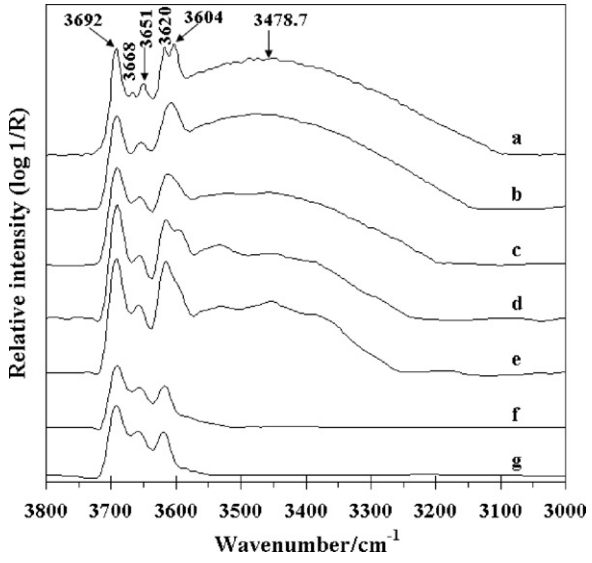


**Fig. 4.** Respective FT-IR spectra of the high frequency region of heating the kaolinite/potassium acetate composite at: (a) room temperature, (b) 150 °C, (c) 200 °C, (d) 250 °C, (e) 300 °C, (f) 350 °C and (g) 400 °C.

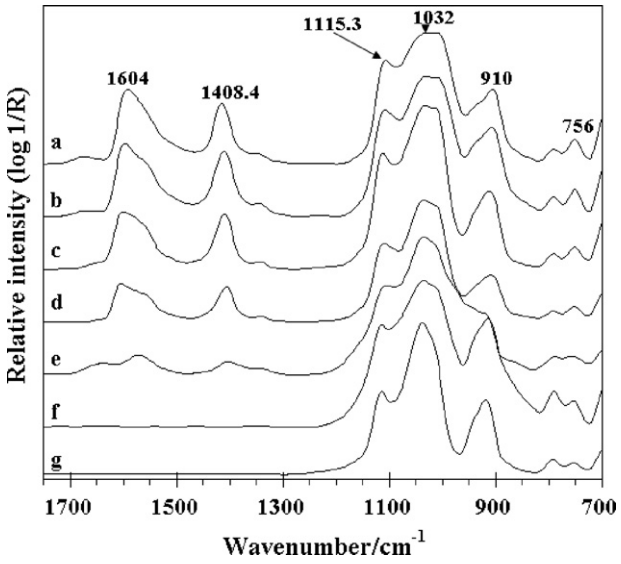


**Fig. 5.** FT-IR spectra of the low frequency region of heating the kaolinite/potassium acetate composite at: (a) room temperature, (b) 150 °C, (c) 200 °C, (d) 250 °C, (e) 300 °C and (f) 350 °C and (g) 400 °C.

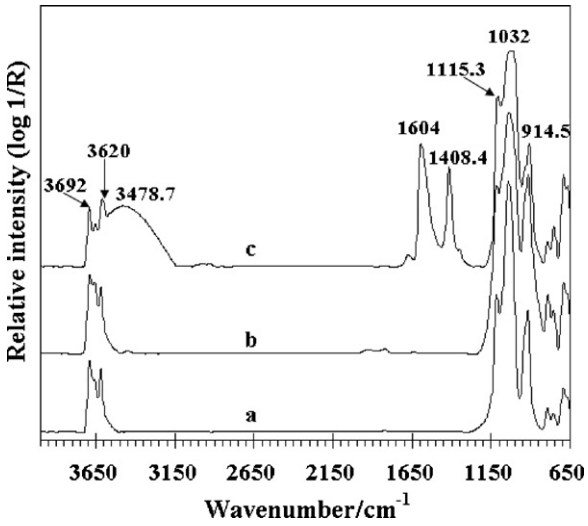


**Fig. 6.** FT-IR spectra of (a) kaolinite, (b) the composite heated at 400 °C and (c) kaolinite/potassium acetate composite.

the lone pair of electrons on the **C=O group. This band disappears when the temperature is above 300 °C (Fig. 4). Such a bond is strong, making the deintercalation difficult except on heating. An additional band at 3478.7 $cm^{-1}$ is observed which is attributed to the hydroxyl stretching frequency of interlayer water coordinated to KAc, and disappears at 350 °C when the temperature increased (Fig. 4f). Upon increasing the temperature, the intensity of the outer surface hydroxyls bands (3668 and 3651 $cm^{-1}$) appear decreased. This decrease in intensity is attributed to the outer surface hydroxyls and hydrogen bonds formed from water and lost when the temperature is raised. The loss of a monolayer of water molecules, presented in the model established by Frost et al. [36,37], would cause a contraction of the basal spacing of the order of 0.23 nm, as observed, e.g. during the loss of water from the kaolinite intercalation composite [20,21] in which the water loss leads to the formation of dehydrated composite with well-defined basal spacing. This observation agrees with the XRD data. At 400 °C, only inner hydroxyls (3620 $cm^{-1}$) and inner surface hydroxyls (3692 $cm^{-1}$) did not change.

The FT-IR spectra of low frequency region of the kaolinite–KAc intercalation composite are show in Fig. 5. When the kaolinite is intercalated with KAc, two additional bands at 1408.4 and 1604 $cm^{-1}$ are observed which are attributed to the vibration peaks of symmetric and antisymmetric stretch vibrations of $CH_3COO^-$. The intense emission bands occurring at 1115.3 $cm^{-1}$ is the Si–O stretching modes which is also decreased when the temperature is raised. This illustrates that the when KAc is actually intercalated into the layer of kaolinite and attached with the inner surface hydroxyl of kaolinite, it will result in the shift of Si–O and Al–O.

Fig. 6 shows the FT-IR spectra of the original kaolinite, the potassium acetate intercalated sample, and the sample heated at 400 °C. In comparison, the KAc intercalation composite decomposes when heated above 400 °C. It is very interesting to observe the disappearance of the 1408.4, 1604 and 3478.7 $cm^{-1}$ bands and the decrease in intensity of the914.5, 1115.3, 3668 and 3651 $cm^{-1}$ band showing a spectral shift towards their original kaolinite. This change is probably associated with the loss of water of hydration of the acetate and potassium ions. The shift in the partially decomposed composite is due to the formation of an intermediate structure and the degradation of deintercalation. The spectra clearly show the decrease in intensity of both the water and the KAc bands as deintercalation takes place. Such results are in accordance with the DSC–TGA and XRD results.

## 4. Conclusion

The DSC–TGA investigation of the intercalation enabled the thermal characteristics of the deintercalation of the KAc intercalated kaolinite to be obtained. Two main changes were observed at 76 and 373 °C, which were attributed to the loss of water and the loss of KAc. The thermal analysis data was used to select appropriate temperatures for the collection of XRD and FT-IR data.

It is proposed that the KAc intercalation composite is stable blew 300 °C except on heating above 300 °C. The two endotherms were observed at 76 and 373 °C. The former attributed to the loss of the water and KAc in the surface of kaolinite and the later attributed to the loss of the KAc in the layer of kaolinite. It was therefore proposed that the outer hydroxyls and hydrogen bonds formed water and loss resulting in the incomplete collapse of the kaolinite structure to the original *d*-spacing. The 3620 $cm^{-1}$ band is attributed to the inner hydroxyl of the kaolinite and shows no change upon deintercalation. Importantly, the 3604 $cm^{-1}$ is attributed to the inner surface hydroxyl of the kaolinite hydrogen-bonded to acetate ions. The structure of the kaolinite was significantly different to its original structure, after deintercalation, at least at the molecular scale.

The maximum rate of dehydroxylation of the intercalation composite is observed at 373 °C, instead of 527 °C, for the pure kaolinite sample. Thus this is benefit to the calcinations. The composite of kaolinite intercalated by KAc prohibits the recrystallization of kaolinite transformed into mullite.

## Acknowledgments

The authors gratefully acknowledge the financial support provided by the National "863" project of China (2008AA06Z109) and the reviewers for their valuable comments that improved the manuscript. The first author also thanks the China Scholarship Council (CSC) for financial support.

## References

[1] H. Ming, Clay Minerals 39 (2004) 349–362.
[2] H.H. Murray, Applied Clay Science 17 (2000) 207–221.
[3] Q. Liu, Y. Zhang, H. Xu, Applied Clay Science 42 (2008) 232–237.
[4] H.H. Murray, I. Wilson, Clays and Clay Minerals 55 (2007) 644–645.

[5] S. Pavlidou, C.D. Papaspyrides, Progress in Polymer Science 33 (2008) 1119–1198.
[6] P. Liu, Applied Clay Science 38 (2007) 64–76.
[7] S. Letaief, P. Aranda, R. Fernandez-Saavedra, J.C. Margeson, C. Detellier, E. Ruiz-Hitzky, Journal of Materials Chemistry 18 (2008) 2227–2233.
[8] J.E. Gardolinski, L.P. Ramos, G.P. de Souza, F. Wypych, Journal of Colloid and Interface Science 221 (2000) 284–290.
[9] F. Franco, M.D. Ruiz Cruz, Clay Minerals 39 (2004) 193–205.
[10] J.E.F.C. Gardolinski, G. Lagaly, Clay Minerals 40 (2005) 547–556.
[11] R.L. Frost, J. Kristof, E. Mako, E. Horvath, Spectrochimica Acta Part A: Molecular and Biomolecular Spectroscopy 59 (2003) 1183–1194.
[12] W. Koji, The American Mineralogist 46 (1961) 78–91.
[13] R.L. Frost, J. Kristof, G.N. Paroz, T.H. Tran, J.T. Kloprogge, Journal of Colloid and Interface Science 204 (1998) 227–236.
[14] M. Janek, K. Emmerich, S. Heissler, R. Nuesch, Chemical Materials 19 (2007) 684–693.
[15] S. Letaief, C. Detellier, Chemistry of Materials 86 (2008) 1–6.
[16] S. Letaief, T.A. Elbokl, C. Detellier, Journal of Colloid Interface Science 302 (2006) 254–258.
[17] I.K. Tonle, T. Diaco, E. Ngameni, C. Detellier, Chemistry of Materials 19 (2007) 6629–6636.
[18] R.L. Frost, J. Kristof, E. Horvath, J.T. Kloprogge, Thermochimica Acta 327 (1999) 155–166.
[19] J. Kristóf, R. Frost, J. Kloprogge, E. Horváth, É. Makó, Journal of Thermal Analysis and Calorimetry 69 (2002) 77–83.
[20] M.D.R. Cruz, F. Franco, Clays and Clay Minerals 48 (2000) 63–67.
[21] M.D.R. Cruz, F. Franco, Clays and Clay Minerals 48 (2000) 586–592.
[22] M. Gabor, M. Toth, J. Kristof, G. Komaromi-Hiller, Clays and Clay Minerals 43 (1995) 223–228.
[23] K. Orzechowski, T. Slonka, J. Glowinski, Journal of Physics and Chemistry of Solids 67 (2006) 915–919.
[24] R.L. Frost, J. Kristof, E. Mako, J.T. Kloprogge, Langmuir 16 (2000) 7421–7428.
[25] J. Kristof, R.L. Frost, W.N. Martens, E. Horvath, Langmuir 18 (2002) 1244–1249.
[26] J. Li, H. Lin, J. Li, J. Wu, Journal of the European Ceramic Society 29 (2009) 2929–2936.
[27] B. Zhang, Y. Li, X. Pan, X. Jia, X. Wang, Journal of Physics and Chemistry of Solids 68 (2007) 135–142.
[28] Y. Deng, G.N. White, J.B. Dixon, Journal of Colloid and Interface Science 250 (2002) 379–393.
[29] R.L. Frost, J. Kristof, G.N. Paroz, J.T. Kloprogge, Journal of Colloid and Interface Science 208 (1998) 216–225.
[30] R.L. Frost, S.J. Van Der Gaast, M. Zbik, J.T. Kloprogge, G.N. Paroz, Applied Clay Science 20 (2002) 177–187.
[31] J. Kristof, R.L. Frost, A. Felinger, J. Mink, Journal of Molecular Structure 410–411 (1997) 119–122.
[32] L.G. Gorb, E.V. Aksenenko, J.W. Adams, S.L. Larson, C.A. Weiss, D. Leszczynska, J. Leszczynski, Journal of Molecular Structure: Theochem 425 (1998) 129–135.
[33] A.C. Hess, V.R. Saunders, The Journal of Physical Chemistry 96 (1992) 4367–4374.
[34] S. Yariv, I. Lapides, Journal of Thermal Analysis and Calorimetry 94 (2008) 433–440.
[35] R.L. Frost, J. Kristof, J.T. Kloprogge, E. Horvath, Journal of Colloid and Interface Science 246 (2002) 164–174.
[36] R.L. Frost, J. Kristof, T.H. Tran, Clay Minerals 33 (1998) 605–617.
[37] R.L. Frost, J. Kristof, G.N. Paroz, J.T. Kloprogge, The Journal of Physical Chemistry B 102 (1998) 8519–8532.